AJG

Article

Overcoming Seasonal Hurdles: Estimating Leaf-on Digital Surface Model from Late Fall LiDAR Data for Enhanced Forest Tree Height Information

Myagmardulam Bilguunmaa*[1] and Kazuyoshi Takahashi [2]

[1]Toyama Prefectural University, Toyama, 939 0398, Japan. Email: <bilguunmaa@pu-toyama.ac.jp>

[2]Nagaoka University of Technology, Niigata, 940 2188, Japan. Email: <ktakaha@vos.nagaokaut.ac.jp>

*Corresponding author: M. Bilguunmaa Email: <bilguunmaa@pu-toyama.ac.jp>

Received: February 16, 2024; Accepted: July 8, 2024; Published: August 3, 2024

ABSTRACT

A canopy height model (CHM) is crucial for effective forest resource assessment, which requires accurate digital surface models (DSMs) during leaf-on periods. This study addresses the challenge of constructing comprehensive CHMs in regions such as Japan, where LiDAR data is predominantly collected in leaf-off seasons. We introduce a novel approach to estimate leaf-on DSMs using late fall LiDAR data, overcoming the limitations of the leaf-off conditions. Our method applies a spatial filtering operation to identify leaf-off grids based on statistical thresholds, followed by a Savitzky-Golay smoothing filter and a local maximum operation for DSM estimation. This innovative technique significantly improved the mean absolute difference (MAD) in DSM estimates, reducing it from 3.2 meters in leaf-off conditions to 1.19 meters for estimated leaf-on conditions. These results demonstrate our approach's potential for year-round forest monitoring and accurate resource assessment, despite the seasonal constraints in LiDAR data collection.

Keywords: Digital Surface Model; Canopy Height Model; DJI Zenmuse l1; LiDAR

1. INTRODUCTION

Forest canopy height information is a fundamental parameter in forest management and carbon emission calculation. Accurate forest height information is important for understanding changes in global impacts on forest ecosystems (Pan et al., 2011). The forest canopy height, a significant parameter in the vertical structure of forests, has been established as a pivotal macroscopic indicator reflecting forest carbon stocks (Zhao et al., 2022). Hence, there is a genuine need for precise quantification of forest canopy height on a large scale in contemporary global carbon balance studies (Giri et al., 2011). Forest canopy height information can be

collected using traditional field surveys, satellite images, and light detection and ranging (LiDAR) technology (Chave et al., 2014; Illarionova et al., 2022; Li Wang, et al., 2020; Lechner et al., 2020; and Guo et al., 2020). Conducting traditional field surveys is demanding in terms of labor and time (Chave et al., 2014). The main advantage of LiDAR measurement lies in its accuracy to capture forest vertical-structure parameters under various conditions, compared to satellite images (Campbell et al., 2021). LiDAR is presently acknowledged as the most precise method for measuring and determining canopy heights (Coops et al., 2021). LiDAR operates by actively emitting laser pulses, relying on the penetration of these pulses to capture three-dimensional point cloud data of vegetation with structural details (Lefsky et al., 2002). Leveraging LiDAR's capacity to capture multiple returns and penetrate forested areas, it enables the generation of both a Digital Elevation Model (DEM) and a Digital Surface Model (DSM). DEM is a three-dimensional representation of the ground surface, excluding above-ground features such as buildings and trees. DSM includes information on above-ground features such as buildings and trees (Song et al., 2023). Canopy Height Models (CHMs) represent the height of trees above the ground topography. Widely used in diverse forestry applications, CHMs play a crucial role in tasks such as monitoring vegetation, computing biomass, and estimating the leaf area index (Hutayanon et al., 2023). The generation of CHM involves subtracting a DEM from a DSM. In Japan, airborne LiDAR observations are often conducted during seasons when trees shed their leaves (leaf-off), such as late fall or winter, to acquire ground surface information. However, when LiDAR data is collected in late fall, the detection of the top of the forest canopy may be incomplete, leading to potential underestimation of the CHM. Nevertheless, the challenge arises in generating a CHM from LiDAR data during these leaf-off seasons due to the incomplete canopy detection. UAVs play a crucial role in forestry, such as mapping forest structures (Zhou et al., 2023; Štroner et al., 2023), measuring tree heights, evaluating tree pruning (Johansen et al., 2018), conducting comprehensive forest inventories (Wallace et al., 2012), and performing various other essential functions in the field (Hartley et al., 2020 and Hu et al., 2020). Cao et al. (2019) found that forest structures in Eastern China were effectively monitored using a multi-rotor GV1300 equipped with a Velodyne Puck VLP-16 laser scanner. Authors in (Wallace et al., 2016) observed forest structure using a Canon 550D digital SLR camera and an Ibeo LUX laser scanner mounted on a Droidworx Skyjib octocopter. (Johansen et al. 2018) investigated tree crop feature extraction with a Parrot Sequoia sensor on a 3DR Solo quadcopter, assessing pruning effects on 189 trees in an Australian lychee

orchard. Forest inventory applications in (Wallace et al., 2012) employed a multi-rotor VTOL UAV OctoCopter Droidworx/Microcopter AD-8 with an Ibeo LUX laser scanner. In Hartley et al. (2020), a young forestry trial survey in New Zealand utilized UAV laser scanning and SfM methods, incorporating a Lidar USA Snoopy V-series system and DJI Matrice 600 Pro UAV. Hu et al. (2020) employed a DJI Matrice 210 UAV for forestry applications, integrating four laser scanners—RIEGL VUX-1 UAV, RIEGL miniVUX-1 UAV, HESAI Pandar40, and Velodyne Puck LITE—showcasing the diverse applications of UAVs in forestry research.

In Zhou et al. (2023), the study investigated how canopy conditions (leaf-on/leaf-off) affect the accuracy of the Ice, Cloud, and Land Elevation Satellite-2 (ICESat-2) forest height estimation. Results reveal better consistency between ICESat-2 and airborne LiDAR terrain heights under leaf-off conditions. Combining ICESat-2 data from both leaf-on and leaf-off seasons improves forest height modeling accuracy, especially when excluding low-quality samples. Štroner et al. (2023) compared the LiDAR-UAV (DJI Zenmuse L1) and Photogrammetric-UAV (DJI Zenmuse P1) systems in a leaf-off forest setting. While photogrammetric data exhibited better elevation accuracy, LiDAR provided superior coverage, emphasizing its effectiveness in dense vegetation. The importance of using multiple returns in LiDAR data processing was highlighted, particularly in areas with high branch density.

The local maximum (LM) algorithm, which begins by identifying individual trees through the detection of maxima, ideally represents treetops. These maxima are determined based on both Canopy Height Model (CHM) values and brightness values (Ke et al., 2011 and Tochon et al., 2015). Challenges arise in defining the search radius for local maxima due to factors such as pixel size, average crown diameter, and the asymmetrical arrangement of tree crowns around a central point in reality (Dietenberger et al., 2023). To improve LM performance, smoothing filters can reduce unwanted noise within the maxima (Workie et al. 2017, Erikson et al., 2005, Hirschmugl et al.,2007, Ottoy et al., 2022). Wulder et al. (2000) found that LM filtering depends on tree size, distribution, and image spatial resolution, with variable window-size techniques reducing errors, especially for larger trees.

In this study, a variable window that dynamically allocates window sizes based on local height for each grid, was employed to address issues in the LM algorithm.

The main objective of this research is to generate an accurate DSM from leaf-off data to improve the overall accuracy of the forest canopy height model in a mixed forest. To enhance the usability of existing leaf-off LiDAR data for forest modeling.

We propose a method that utilizes raster DSM data, divided into two categories: leaf-off and leaf-on condition grids. To reduce commission errors and enhance the accuracy of LM performance, we have proposed an LM algorithm method specifically for leaf-off grids while applying a smoothing filter (a Modified Savitzky-Golay) for leaf-on grids. In addition, the proposed method was evaluated using leaf-on condition experimental data acquired in August.

2. DATA AND METHODS

2.1 Experimental setup

The field experiment was conducted at Gohen-no-mizube park along the Shinano River in Ojiya-shi, Niigata Prefecture, located on the island of Honshū on the coast of the Sea of Japan. The leaf-on data, gathered in August 2022, deliver comprehensive insights into the vegetative cover, offering critical details about the height and density of the forested area. In contrast, the leaf-off data, obtained in December 2022, complements this by capturing a different perspective during a period when the vegetation sheds its leaves. The dominant tree species were False Acacia. The DJI Zenmuse L1 represents a cutting-edge laser scanner that integrates data from both an RGB sensor and an Inertial Measurement Unit (IMU) within a stabilized 3-axis gimbal. This innovative setup allows for the simultaneous capture of synchronized point clouds and images, enabling the creation of vivid, true-color point clouds derived from the RGB sensor. Operating at a wavelength of 905 nm and a frequency of 48 kHz, this laser scanner provides precise data when mounted on the DJI Matrice 300 drone. The details of the measurement setup are shown in Figure 1. A map of the study area is shown in Figure 1(a). In Figure 1(b), the light blue rectangle indicates the location of the leaf-on and leaf-off data. Figures 1(c) and 1(d) show the DJI Matrice 300 drone and DJI Zenmuse L1 lidar sensor, respectively, used in this study. The specifications of the experimental setup are listed in Table I.

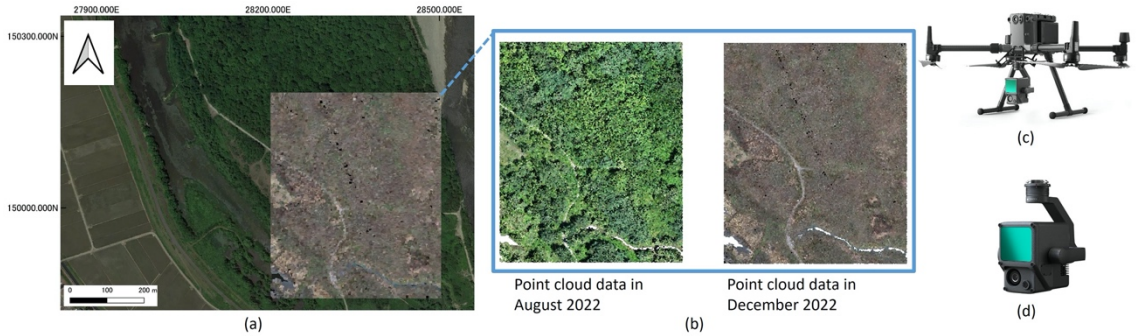

Figure 1: Experimental setup: (a) Map of study area; (b) data used in this study; (c) DJI Matrice 300 drone; (d) DJI Zenmuse L1 sensor.

Table I: Experimental setup.

Description	Value
Platform	DJI Matrice 300 RTK
Flight attitude	80 m
Flight speed	10 m/s
Flight time	9 min
LiDAR Sensor	DJI Zenmuse L1
Dimensions	152 × 110 × 169 mm
Weight	930 ± 10 g
Range	450 m @ 80% reflectivity, 190 m @ 10% reflectivity
Point data rate/Scan mode	Multiple return: max. 480,000 pts/s /repetitive
Positional Accuracy	Horizontal: 10 cm @50 m, Vertical: 5 cm @50 m
Ranging Accuracy	3 cm @100 m

2.2 LiDAR point cloud data to raster DSM generation

Various software is available to generate DSM and DEM from different data sources. In this study, DSMs were generated from LiDAR point cloud (leaf-off) and leaf-on (reference). The DSM is computed by the highest point measured in each pixel. In the generation of DSM and DEM from LiDAR point cloud data, a filtering strategy was implemented wherein values greater than -99999 were designated for DSM, and values less than 99999 were assigned to DEM. This delineation was encoded into the C++ source code to facilitate data processing. The threshold values of -99999 and 99999 are commonly employed as placeholders to signify 'No-Data' within geographical data processing. By establishing such thresholds, the goal is to effectively exclude these No-Data values from the calculations that produce the DSM and DEM, ensuring the accuracy and reliability of the resulting models. Point cloud data is converted to raster data. The values of the raster cells were set to the height of the highest point within each cell. If no point lies within a cell, the raster value was left empty (no data). Generating a DSM (DEM) with a small grid size, such as 0.1 m, results in "No-Data" grids that do not contain any points. On the other hand, increasing the grid size reduces "No-Data" grids, but ground surface or tree shape information is lost. Therefore, we generated DSMs from leaf-on and leaf-off point clouds by varying the grid size from 0.1 m to 5 m and determined the grid size for analysis based on the Mean Absolute Difference (MAD) of both DSMs and the number of points in the grid.

2.3 Extraction of leaf-off grids

We employed a statistical approach to extract grids to apply estimation processes. In this study, it is assumed that a tree crown surface in leaf-on is very smooth, but the surface of leaf-off trees is very rough. A standard deviation of a DSM value in leaf-on areas is expected to be low. In contrast, it is expected that the standard deviation of a DSM value in leaf-off areas might be high. Leaf-off grids can be defined using local standard deviation. Therefore, to discriminate between grids corresponding to both leaf-on and leaf-off conditions, we sampled data from local standard deviation values of the DSM, which were calculated with various window sizes. In the literature, the utilization of the standard deviation in the calculation of sigma clipping has been highlighted as a method for identifying cloud cover and extracting clear sky radiances (Coakley et al., 1982). The

standard deviation was calculated using equation (1).

$$\sigma_{ij} = \sqrt{\frac{\sum_{k=-W/2}^{W/2}\sum_{l=-W/2}^{W/2}\left(x_{i+k\,j+l}-\bar{x}_{ij}\right)^2}{(W)^2}} \quad (1)$$

Here, W is the window size; $x_{i+k,j+l}$ is the grid value at position $(i+k, j+l)$ within the local window; $\bar{x}_{ij}$ is the mean average grid value within the local window centered at (i, j), and σ is the standard deviation.

After the computation, distinct standard deviation threshold values were determined for leaf-off and leaf-on conditions.

2.4 Proposed DSM generation method

For the grids extracted by the process described in the previous section, the estimated DSM value was calculated using modified Savitzky-Golay (MSG) and Local Maximum (LM) algorithms. Figure 2 shows the data flow diagram of the estimation of the leaf-on DSM task framework of this study. The smoothing filter is applied only in leaf-on grids, while leaf-off grids and canopy gap grids are excluded from the MSG calculation, so it is expected to reduce the canopy gap area. It is expected that the data sets may provide more helpful information in predicting tree growth and less underestimated productivity.

The LM filtering method was applied to the leaf-off grids, while the MSG smoothing filter was used for the leaf-on grids around leaf-off grids. LM is a technique for calculating the highest value of a grid based on the number of calculation grid cells (window size). It assigns the output cell value by taking the highest value of the calculation window size in an image to generate new values. If DSM is generated from the LiDAR data in leaf-off conditions, it may represent tree trunks and branches, and thus the LM value may be expected to represent tree crown surfaces.

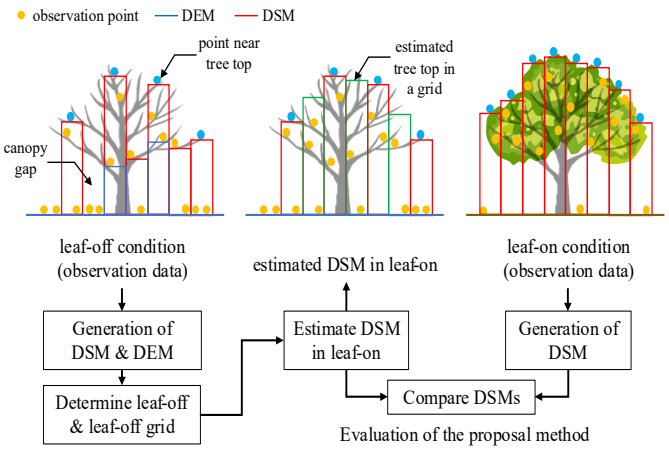

Figure 2: Data flow diagram of estimation of leaf-on DSM task framework.

2.4.1 Savitzky-Golay data smoothing filtering and local maximum

A Savitzky-Golay (SG) filter is a digital filter that can be applied to a set of digital data points for the purpose of smoothing the data, that is, to increase and decrease data without greatly distorting the data. The SG filter is a type of digital filter used primarily for data smoothing, fitting a low-order polynomial by the method of least squares to a successive subset of adjacent data points (Savitzky et al., 1964). The key idea is that the smoothed value Y^* in the point C_i is obtained by taking an average of the neighboring data. Caused by the smoothing, the risk exists to overestimate the canopy gap area. The overall equation for the simplified quadratic surface applied to smooth DSM data can be expressed as follows (Chen et al., 2004).

$$Y_j^* = \frac{\sum_{i=-m}^{i=m} C_i Y_{j+i}}{N} \quad (2)$$

Here, Y is the original data value, Y^* is the smoothed value, C_i is the coefficient for the ith data value of the filter (smoothing window), and N is the number of convoluting integers and is equal to the smoothing window $(2M+1)$. The index j is the running index of the original ordinate data. The smoothing array (filter size) consists of $2M+1$ points, where m is the half-width of the smoothing window.

In this study, a quadratic surface is used for data smoothing. In order to minimize overestimation, a smoothing filter is used based on extraction from leaf-off grids. A Savitzky–Golay filter is applied for extracted leaf-on grids around leaf-off grids. It is called a Modified Savitzky–Golay (MSG) filter. It is expected that there will be less overestimation in the canopy gap area. MSG filter functions through a process of local least squares approximation to effectively filter the noise signal (Schafer et al., 2011). The local polynomial is mathematically represented as follows, where a data frame encompasses a total of $2M+1$ sample points centered at $n=0$:

$$p(n) = \sum_{k=0}^{N} a_k n^k \quad (3)$$

where $N(N \leq 2M+1)$ is the power of the polynomial.

The general form of an MSG filter is based on fitting a polynomial to the data with a moving window. The equation for a quadratic surface in the context of the modified MSG filter can be expressed as follows:

$$Z = av^2 + bv + cw^2 + dw + e \quad (4)$$

where Z is the estimated elevation value, and v and w represent the coordinates in the x and y directions, respectively. The coefficients a, b, c, d and e are determined by the filter based on the data within the moving window. The MSG filter uses linear algebra to solve the system of equations formed by the polynomial terms and the observed elevation values within the calculation

window.

LM algorithm was introduced to detect treetops. The main problem encountered when using LM to detect treetops is that non-treetop LM are incorrectly classified as treetops. LM is a method to estimate tree heights based on single tree identification. A common technique used to identify tree locations on high/resolution optical images uses a LM algorithm with a static-sized, user specified, moving window, commonly 3x3, 5x5, 7x7, 9x9 and 11x11 pixels, depending also on the pixel size (Nieman et al., 1998 and Gougen et al., 2002).

2.5 Evaluation of the proposed model

In this study, the mean absolute difference (MAD) is calculated to evaluate the proposed method's results. The difference between the reference DSM and estimated DSM is evaluated based on the MAD, which was calculated as:

$$MAD = \frac{1}{n}\sum_{i=1}^{n}|x_i - y_i| \quad (5)$$

Here, x_i and y_i are the values of the estimated and measured DSM data, and n is the total amount of data.

3. RESULTS

3.1 Generation of DSM and DEM

The DSMs were generated with grid sizes of 0.1, 0.2, 0.25, 0.5, 1.0, 1.5, 2.0, 3.0, 4.0, and 5.0 meters. The MAD values were calculated for each generated DSM, and the results are shown in Figure 3. The MAD values for DSMs with grid sizes greater than 1.0 meter were nearly constant, ranging from 1.35 meters to 0.65 meters. This indicates that DSMs with grid sizes greater than 1.0 meter could not capture the leaf-off information. For data with grid sizes of 0.1, 0.2, 0.25, 0.5, and 1.0 meters, the point grid ratios were calculated. The results are listed in Table II. For this study, we used a grid size of 0.2 m instead of 0.1 m, which would have resulted in a point count in the grid of less than 10 (the number of points in the grid was 22 with a 0.2 m grid). A grid size of 0.2 meters and a MAD value of 3.2 meters were chosen to generate both DSMs.

Figure 4 shows (a) the reference DSM data with a resolution of 0.2 m and (b) the leaf-off DSM data, respectively. The process involved analyzing the number of points in each grid, as well as the ratio of "No-Data" grids in the target area and the mean absolute difference (MAD).

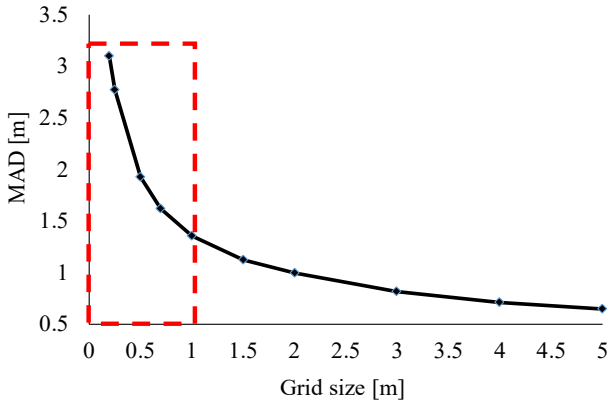

Figure 3: Mean Absolute Differences (MAD) between DSMs generated from point clouds of both leaf-on and leaf-off observations.

Table II. Mean number of points in the grid with various grid sizes.

Grid size [m]	0.1	0.2	0.25	0.5	1.0
Mean point density [points/m^2]	5.6	22	35	140	563

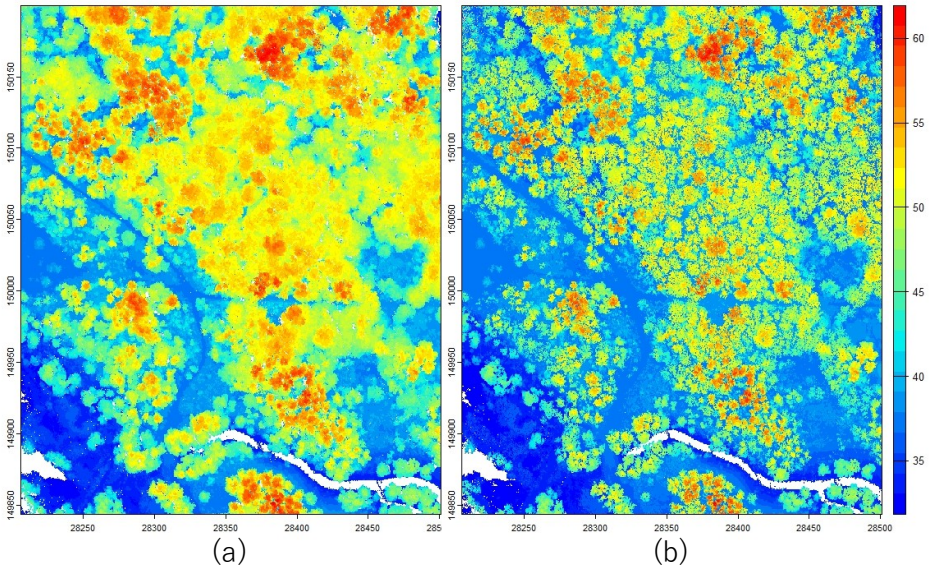

Figure 4: Generated DSM and DEM results with grid size of 0.2 m; (a) Reference leaf-on DSM in August, (b) leaf-off DSM data in December.

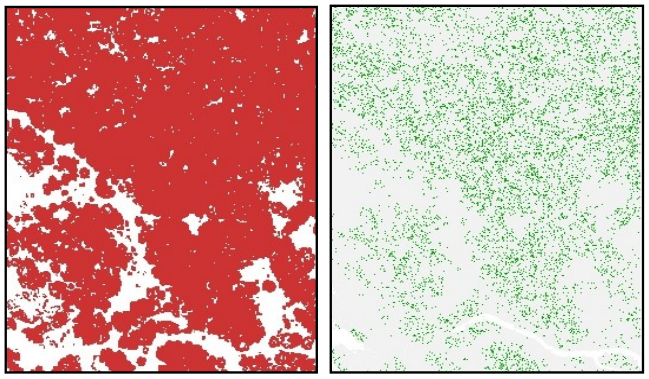

(a)Leaf-off grids (b)Leaf-on grids

Figure 5: (a) red colored area is leaf-off grids for the applying the estimation method, (b) leaf-on grids (green colored) to excluded from MSG filter.

3.2 Determination of leaf-on and leaf-off grids

Figure 5 shows the results of the leaf-on and leaf-off grids. Based on the leaf-off DSM, we computed the local standard deviation of the image data using different window sizes (3x3, 5x5, and 7x7).

The extraction of leaf-off grids was contingent on factors such as window size, tree crown size, tree distributions, and a specified threshold. In the present study, the threshold was established using both the MAD values and visual comparison with the extracted grids against the leaf-off DSM and reference DSM. The study, which relies on the standard deviation for parameter optimization, has identified that a 5x5 window size and a threshold of 2.0 meters are optimal for extracting leaf-off grids in the area. By selecting a 5x5 window size, the study ensures a balanced consideration of neighboring pixels when computing local differences, thus capturing meaningful spatial relationships without excessive smoothing or oversimplification. Additionally, the threshold of 2.0 meters provides a reasonable criterion for identifying significant changes in elevation data. This optimal parameter combination reflects a careful balance between spatial resolution and sensitivity to variations in the dataset.

3.3 Results of Estimated DSM in leaf-on season

Figure 6 shows the results of (a) Leaf-on DSM in August, (b) leaf-off DSM data in December, and (c) the result of estimated leaf-on DSM in December. The estimated DSMs were generated through Modified Savitzky-Golay filtering and LM processes, employing various window sizes (3, 5, 7, 9 and 11). Among the window sizes tested, the 5x5 window size emerged as optimal for both smoothing and LM identification. It exhibited the lowest MAD values for both techniques, indicating superior performance. This suggests that a balance between the size of the neighborhood considered and the resolution of the features in the data is crucial for achieving optimal results. The first method estimates values based on a

modified Savitzky-Golay filter (MSG), involving a more complex computation as it utilizes the MSG function to estimate values for target grid cells based on surrounding data in the original DSM. The second method estimates values directly from the LM data. It simply retrieves the values from the calculated LM dataset for target grid cells. The LM algorithm in the target area favored the window size (5x5) for crown surface estimation. This suggests that employing a small smoothing window size in MSG filtering enhances the accuracy of the filtered values.

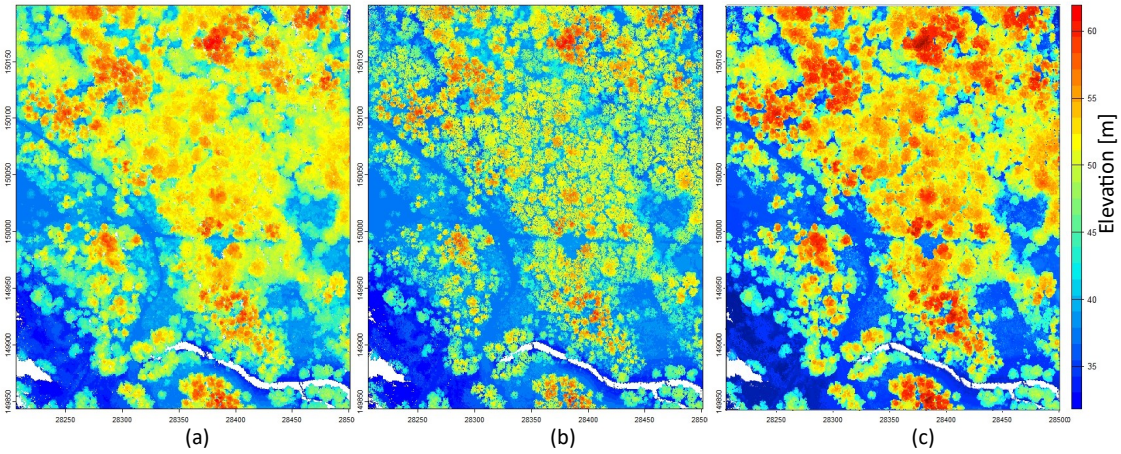

Figure 6. (a) leaf-on DSM in August, (b) leaf-off DSM data in December, (c) result of estimated leaf-on DSM in December.

3.4 Evaluation of proposed method

The reference DSM data were generated from the leaf-on season data. Any grids that contain "No-Data" values were excluded when evaluating the estimated DSM and reference DSM data. The window sizes were refined based on their shapes and distance between treetops. The evaluation of all estimated DSMs has been shown in Table III. A minimum MAD value of 1.19 m occurred at the window size of 5x5. Table III represents the analysis of MAD values for the LM and MSG filtering processes with varying window sizes (3x3, 5x5, 7x7, 9x9, and 11x11), providing valuable insights into the performance of the filtering technique. The observed MAD values for the MSG filter (3.10, 2.44, 2.37, 2.35, and 2.36, respectively) and for the LM algorithm (1.49, 1.19, 1.27, 1.48, and 1.68, respectively) provide insights into the dispersion or variability present in the filtered data across different tree species and growth sizes. Figure 7, parts (a) and (b) represent a comparison of DSM and DEM cross-sections. From the results in Figure 7, parts (a) and (b), it is obvious that the DSM successfully estimates tree height surface information for the available details in leaf-off areas. Figure 7 shows that the estimation process in the leaf-off region has good accuracy. A smoothing filter reduced the overestimation in the

canopy gap area because the proposed smoothing method was applied only to leaf-on grids, excluding leaf-off grids from the MSG process.

4. DISCUSSION

This study estimated the DSM and compared the original DSM profiles with the reference DSM profiles. Figure 7 compares the DSM and DEM data profiles, with a depth of 0.2 m, before and after estimation. The MSG filter produced a better surface compared with the original LiDAR, especially under the tree canopy gap area (Figure 7). The results have shown that this methodology reduced overestimation. When generating various DSM data, the grid size should be adapted depending on the nature of the target and terrain features, such as crown size and tree distributions. Parameter adjustment of the MSG filter calculation successfully removed canopy gap points in this area. It is clear that the canopy gap area has improved, and other areas match the reference data. As a result of comparing the MADs of both the estimated DSM and the reference DSM, a DSM in leaf-on conditions could be estimated from leaf-off LiDAR data using our proposed method. A higher MAD value indicates greater dispersion or variability in the filtered data. In the case of MSG, the observed MAD values (ranging from 2.44 to 3.10) suggest varying degrees of dispersion, possibly influenced by factors such as tree species composition, terrain characteristics, and the overall complexity of the landscape. On the other hand, the MAD values for the LM algorithm (ranging from 1.19 to 1.68) also demonstrate variability in the filtered data but generally exhibit lower dispersion compared to MSG. This suggests that the LM algorithm tends to produce smoother results with less variation in elevation values. The discussion underscores the significance of MAD values in evaluating filtering outcomes and guides further considerations for refining the filtering parameters in future applications.

Table III: MAD value of estimated DSM with various window size.

Window size	MAD [m]		
	original	Modified SG	LM
3x3	3.20	3.10	1.49
5x5	3.20	2.44	1.19
7x7	3.20	2.37	1.27
9x9	3.20	2.35	1.48
11x11	3.20	2.36	1.68

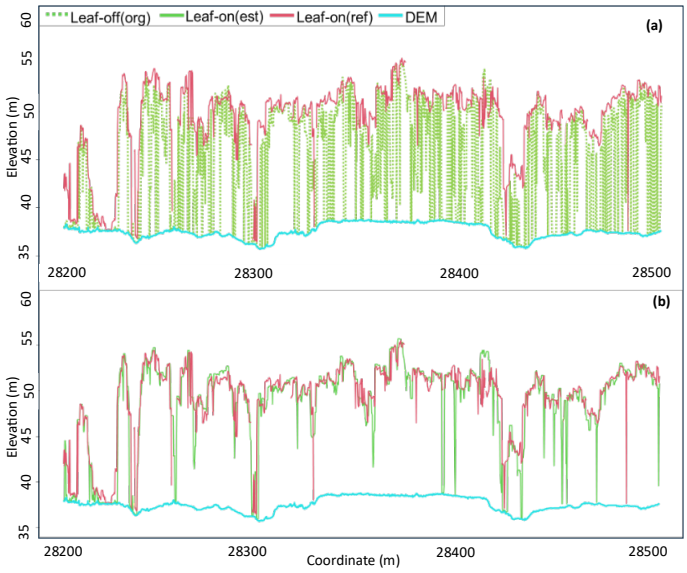

Figure 7: Sample of DSM and DEM data profiles with the depth of 0.2 m are compared, (a) before estimation and (b) after estimation.

5. CONCLUSION

In this study, we presented a method for developing a DSM in leaf-on condition, based on the combination of LM and MSG smoothing filters, using grids extracted from leaf-off LiDAR data in Niigata, Japan. We confirmed that the estimation method of the leaf-off grids with a combination of the LM and MSG smoothing filter showed better performance. The estimated DSM results were validated using the actual reference leaf-on DSM data.

Leaf-off grids can be extracted from local standard deviation data of the original DSM with a 5x5 window size and a threshold of 2.0 m. In extracted grids, a DSM in leaf-on was estimated using a 5x5 window size of the LM filtered data. The original MAD value of 3.2 m for the leaf-off DSM was decreased to 1.19 m in the leaf-on DSM estimation. We improved the overall accuracy of the estimated DSM with an average of 2 meters for the experimental data. The grid size of the estimation process should be changed depending on the nature of the target area, such as crown size and tree distributions. Based on the results, our proposed method is well suited for improving the practical applicability of available leaf-off data in a mixed forest environment. The proposed method is suitable for different types of trees and forests, where the density of the forest presents the most significant challenge.

ACKNOWLEDGMENTS

The authors thank Mr. Takeshi Nakamura, a technician at Nagaoka University of Technology, for acquiring the point cloud data of the forest.

REFERENCES

Campbell, Michael J., Philip E. Dennison, Kelly L. Kerr, Simon C. Brewer, and William R.L. Anderegg. 2021. "Scaled Biomass Estimation in Woodland Ecosystems: Testing the Individual and Combined Capacities of Satellite Multispectral and Lidar Data." *Remote Sensing of Environment* 262 (112511): 112511. https://doi.org/10.1016/j.rse.2021.112511.

Cao, Lin, Hao Liu, Xiaoyao Fu, Zhengnan Zhang, Xin Shen, and Honghua Ruan. 2019. "Comparison of UAV LiDAR and Digital Aerial Photogrammetry Point Clouds for Estimating Forest Structural Attributes in Subtropical Planted Forests." *Forests* 10 (2): 145. https://doi.org/10.3390/f10020145.

Chave, Jérôme, Maxime Réjou-Méchain, Alberto Búrquez, Emmanuel Chidumayo, Matthew S. Colgan, Welington B.C. Delitti, Alvaro Duque, et al. 2014. "Improved Allometric Models to Estimate the Aboveground Biomass of Tropical Trees." *Global Change Biology* 20 (10): 3177–90. https://doi.org/10.1111/gcb.12629.

Chen, Jin, Per. Jönsson, Masayuki Tamura, Zhihui Gu, Bunkei Matsushita, and Lars Eklundh. 2004. "A Simple Method for Reconstructing a High-Quality NDVI Time-Series Data Set Based on the Savitzky–Golay Filter." *Remote Sensing of Environment* 91 (3-4): 332–44. https://doi.org/10.1016/j.rse.2004.03.014.

Coakley, James A., and Francis P. Bretherton. 1982. "Cloud Cover from High-Resolution Scanner Data: Detecting and Allowing for Partially Filled Fields of View." *Journal of Geophysical Research* 87 (C7): 4917. https://doi.org/10.1029/jc087ic07p04917.

Coops, Nicholas C., Piotr Tompalski, Tristan R. H. Goodbody, Martin Queinnec, Joan E. Luther, Douglas K. Bolton, Joanne C. White, Michael A. Wulder, Oliver R. van Lier, and Txomin Hermosilla. 2021. "Modelling Lidar-Derived Estimates of Forest Attributes over Space and Time: A Review of Approaches and Future Trends." *Remote Sensing of Environment* 260 (112477): 112477. https://doi.org/10.1016/j.rse.2021.112477.

Erikson, Mats, and Kenneth Olofsson. 2005. "Comparison of Three Individual Tree Crown Detection Methods." *Machine Vision and Applications* 16 (4): 258–65. https://doi.org/10.1007/s00138-005-0180-y.

Giri, C., E. Ochieng, L. L. Tieszen, Z. Zhu, A. Singh, T. Loveland, J. Masek, and N. Duke. 2010. "Status and Distribution of Mangrove Forests of the World Using Earth Observation Satellite Data." *Global Ecology and Biogeography* 20 (1): 154–59. https://doi.org/10.1111/j.1466-8238.2010.00584.x.

Gougeon, François A, and Donald G Leckie. 2001. "Individual Tree Crown Image Analysis - a Step towards Precision

Forestry ∗." *Proceedings of the First International Precision Forestry Cooperative Symposium (P. 43). Institute of Forest Resources, College of Forest Resources, University of Washington.*, January.

Guillaume Tochon, Jean-Baptiste Féret, Silvia Valero, R M Martin, D J Knapp, Philippe Salembier, Jocelyn Chanussot, and Gregory P Asner. 2015. "On the Use of Binary Partition Trees for the Tree Crown Segmentation of Tropical Rainforest Hyperspectral Images." *Remote Sensing of Environment* 159 (318-331): 318–31. https://doi.org/10.1016/j.rse.2014.12.020.

Guo, Qinghua, Yanjun Su, Tianyu Hu, Hongcan Guan, Shichao Jin, Jing Zhang, Xiaoxia Zhao, et al. 2021. "Lidar Boosts 3D Ecological Observations and Modelings: A Review and Perspective." *IEEE Geoscience and Remote Sensing Magazine* 9 (1): 232–57. https://doi.org/10.1109/mgrs.2020.3032713.

Hartley, Robin J. L., Ellen Mae Leonardo, Peter Massam, Michael S. Watt, Honey Jane Estarija, Liam Wright, Nathanael Melia, and Grant D. Pearse. 2020. "An Assessment of High-Density UAV Point Clouds for the Measurement of Young Forestry Trials." *Remote Sensing* 12 (24): 4039. https://doi.org/10.3390/rs12244039.

Hirschmugl, Manuela, Martina Franke, Martin Ofner, Mathias Schardt, and Hannes Raggam. 2005. "Single Tree Detection in Very High Resolution Remote Sensing Data." *Proc. Of ForestSat* , January.

Hu, Tianyu, Xiliang Sun, Yanjun Su, Hongcan Guan, Qianhui Sun, Maggi Kelly, and Qinghua Guo. 2020. "Development and Performance Evaluation of a Very Low-Cost UAV-Lidar System for Forestry Applications." *Remote Sensing* 13 (1): 77. https://doi.org/10.3390/rs13010077.

Illarionova, Svetlana, Dmitrii Shadrin, Vladimir Ignatiev, Sergey Shayakhmetov, Alexey Trekin, and Ivan Oseledets. 2022. "Estimation of the Canopy Height Model from Multispectral Satellite Imagery with Convolutional Neural Networks." *IEEE Access* 10 (34116-34132): 34116–32. https://doi.org/10.1109/access.2022.3161568.

Johansen, Kasper, Tri Raharjo, and Matthew McCabe. 2018. "Using Multi-Spectral UAV Imagery to Extract Tree Crop Structural Properties and Assess Pruning Effects." *Remote Sensing* 10 (6): 854. https://doi.org/10.3390/rs10060854.

Ke, Yinghai, and Lindi J. Quackenbush. 2011. "A Review of Methods for Automatic Individual Tree-Crown Detection and Delineation from Passive Remote Sensing." *International Journal of Remote Sensing* 32 (17): 4725–47. https://doi.org/10.1080/01431161.2010.494184.

Lechner, Alex M., Giles M. Foody, and Doreen S. Boyd. 2020. "Applications in Remote Sensing to Forest Ecology and Management." *One Earth* 2 (5): 405–12.

https://doi.org/10.1016/j.oneear.2020.05.001.

Lefsky, Michael A., Warren B. Cohen, David J. Harding, Geoffrey G. Parker, Steven A. Acker, and S. Thomas Gower. 2002. "Lidar Remote Sensing of Above-Ground Biomass in Three Biomes." *Global Ecology and Biogeography* 11 (5): 393–99. https://doi.org/10.1046/j.1466-822x.2002.00303.x.

Li, Wang, Zheng Niu, Rong Shang, Yuchu Qin, Li Wang, and Hanyue Chen. 2020. "High-Resolution Mapping of Forest Canopy Height Using Machine Learning by Coupling ICESat-2 LiDAR with Sentinel-1, Sentinel-2 and Landsat-8 Data." *International Journal of Applied Earth Observation and Geoinformation* 92 (102163): 102163. https://doi.org/10.1016/j.jag.2020.102163.

Ottoy, Sam, Nikolaos Tziolas, Koenraad Van Meerbeek, Ilias Aravidis, Servaas Tilkin, Michail Sismanis, Dimitris Stavrakoudis, Ioannis Z Gitas, George Zalidis, and Alain De Vocht. 2022. "Effects of Flight and Smoothing Parameters on the Detection of Taxus and Olive Trees with UAV-Borne Imagery." *Drones* 6 (8): 197–97. https://doi.org/10.3390/drones6080197.

Pan, Y., R. A. Birdsey, J. Fang, R. Houghton, P. E. Kauppi, W. A. Kurz, O. L. Phillips, et al. 2011. "A Large and Persistent Carbon Sink in the World's Forests." *Science* 333 (6045): 988–93. https://doi.org/10.1126/science.1201609.

Savitzky, Abraham., and M. J. E. Golay. 1964. "Smoothing and Differentiation of Data by Simplified Least Squares Procedures." *Analytical Chemistry* 36 (8): 1627–39. https://doi.org/10.1021/ac60214a047.

Schafer, Ronald. 2011. "What Is a Savitzky-Golay Filter? [Lecture Notes]." *IEEE Signal Processing Magazine* 28 (4): 111–17. https://doi.org/10.1109/msp.2011.941097.

Song, Hunsoo, and Jinha Jung. 2023. "An Object-Based Ground Filtering of Airborne LiDAR Data for Large-Area DTM Generation." *Remote Sensing* 15 (16): 4105–5. https://doi.org/10.3390/rs15164105.

Steffen Dietenberger, Marlin M Mueller, Felix Bachmann, Maximilian Nestler, Jonas Ziemer, Friederike Metz, Marius G Heidenreich, et al. 2023. "Tree Stem Detection and Crown Delineation in a Structurally Diverse Deciduous Forest Combining Leaf-on and Leaf-off UAV-SfM Data." *Remote Sensing* 15 (18): 4366–66. https://doi.org/10.3390/rs15184366.

Štroner, Martin, Rudolf Urban, Tomáš Křemen, and Jaroslav Braun. 2023. "UAV DTM Acquisition in a Forested Area – Comparison of Low-Cost Photogrammetry (DJI Zenmuse P1) and LiDAR Solutions (DJI Zenmuse L1)." *European Journal of Remote Sensing* 56 (1). https://doi.org/10.1080/22797254.2023.2179942.

T., G. Workie. 2017. "Estimating Forest Above-Ground Carbon Using Object-Based Analysis of Very High Spatial Resolution Satellite Images." *African Journal of Environmental Science and Technology* 11 (12): 587–600. https://doi.org/10.5897/ajest2017.2358.

Thitinan Hutayanon, and Komsoon Somprasong. 2023. "Application of Integrated Spatial Analysis and NDVI for Tree Monitoring in Reclamation Area of Coal Mine." *Environmental Science and Pollution Research* 1-11 (111). https://doi.org/10.1007/s11356-023-28910-1.

Wallace, Luke, Arko Lucieer, Zbyněk Malenovský, Darren Turner, and Petr Vopěnka. 2016. "Assessment of Forest Structure Using Two UAV Techniques: A Comparison of Airborne Laser Scanning and Structure from Motion (SfM) Point Clouds." *Forests* 7 (12): 62. https://doi.org/10.3390/f7030062.

Wallace, Luke, Arko Lucieer, Christopher Watson, and Darren Turner. 2012. "Development of a UAV-LiDAR System with Application to Forest Inventory." *Remote Sensing* 4 (6): 1519–43. https://doi.org/10.3390/rs4061519.

Wulder, Mike, K. Olaf Niemann, and David G. Goodenough. 2000. "Local Maximum Filtering for the Extraction of Tree Locations and Basal Area from High Spatial Resolution Imagery." *Remote Sensing of Environment* 73 (1): 103–14. https://doi.org/10.1016/S0034-4257(00)00101-2.

Zhao, Meifang, Mengde Sun, Tao Xiong, Shihong Tian, and Shuguang Liu. 2022. "On the Link between Tree Size and Ecosystem Carbon Sequestration Capacity across Continental Forests." *Ecosphere* 13 (6). https://doi.org/10.1002/ecs2.4079.

Zhou, Jialu, Yunyuan Deng, Sheng Nie, Jing Fu, Cheng Wang, Wenwu Zheng, and Yue Sun. 2023. "Effect of Leaf-on and Leaf-off Canopy Conditions on Forest Height Retrieval and Modelling with ICESat-2 Data." *International Journal of Digital Earth* 16 (2): 4831–47. https://doi.org/10.1080/17538947.2023.2285807.